IOPscience iopscience.iop.org

Home Search Collections Journals About Contact us My IOPscience

Electron-beam-induced current study of electrically active defects in 4H-SiC

This article has been downloaded from IOPscience. Please scroll down to see the full text article.

2004 J. Phys.: Condens. Matter 16 S217

(http://iopscience.iop.org/0953-8984/16/2/026)

View the table of contents for this issue, or go to the journal homepage for more

Download details:
IP Address: 129.252.86.83
The article was downloaded on 28/05/2010 at 07:16

Please note that terms and conditions apply.

J. Phys.: Condens. Matter **16** (2004) S217–S223 PII: S0953-8984(04)66989-X

Electron-beam-induced current study of electrically active defects in 4H-SiC

C Díaz-Guerra and J Piqueras

Departamento de Física de Materiales, Facultad de Físicas, Universidad Complutense de Madrid, Ciudad Universitaria s/n, E-28040 Madrid, Spain

Received 31 July 2003
Published 22 December 2003
Online at stacks.iop.org/JPhysCM/16/S217 (DOI: 10.1088/0953-8984/16/2/026)

Abstract
Electrically active defects in epitaxial, n-type, 4H-SiC have been investigated by electron-beam-induced current (EBIC) in the scanning electron microscope. Several defects, mainly nanopipes, 6H polytype inclusions and triangular, carrot-like, defects were detected by different techniques, including atomic force microscopy and cathodoluminescence. However, EBIC images reveal that only nanopipes are electrically active. The hole diffusion length (L) was calculated at different temperatures from EBIC line scans recorded in defect-free regions. L values of 3.1 ± 0.2 and 4.8 ± 0.3 μm were respectively estimated at 295 and 420 K. A strong decrease of the diffusion length was observed in the proximity of the nanopipes.

1. Introduction

In the last decade, SiC has received renewed attention as a suitable material for high-power and high-frequency devices requiring high-temperature operation [1, 2]. The inherent properties of SiC, such as large breakdown electric field strength, large electron drift velocity, small dielectric constant, high thermal conductivity and its capability to work in harsh environments, makes SiC an attractive candidate in applications for which GaAs and Si are not adequate [3]. Unfortunately, large defect densities have prevented the widespread use of SiC in commercial high-power applications so far, although a significant improvement in the epitaxial material quality has been recently achieved. In particular, the micropipe density has been used as the foremost indicator of material quality, although it is recognized that other defects may also influence the electrical characteristics of SiC-based devices [4, 5].

Both native defects and impurities in SiC create recombination centres which reduce the local generation/recombination lifetimes of charge carriers and may affect the device performance. Spatially resolved, non-destructive, characterization techniques are thus required for defect and doping inhomogeneity assessment of epitaxial layers.

In this work, cathodoluminescence (CL) in the scanning electron microscope (SEM) has been used to investigate the nature and spatial distribution of defects in epitaxial, n-type, 4H-SiC doped with N.

0953-8984/04/020217+07$30.00 © 2004 IOP Publishing Ltd Printed in the UK

The existence of several defects, mainly nanopipes with sizes ranging from 250 to 900 nm, 6H polytype inclusions and triangular, carrot-like, defects was also revealed by atomic force microscopy (AFM) and CL in the SEM.

2. Experimental details

Schottky diodes were fabricated by Au evaporation on a N-doped ($n = 2 \times 10^{15}$ cm^{-3}), 30 μm thick, 4H-SiC epitaxial layer from CREE Research [6]. This epilayer was grown on a 1 μm thick buffer layer ($n = 1 \times 10^{18}$ cm^{-3}) deposited on the Si face of a heavily doped ($n = 6.8 \times 10^{18}$ cm^{-3}), 320 μm thick, 4H-SiC substrate. The Ohmic contact was fabricated by Ti/Pt/Au electron-beam deposition on the backside of the structure. Schottky contacts in cross-section configuration were obtained by gold evaporation covering the first two layers and part of the substrate.

Electron-beam-induced current (EBIC) observations were performed in a Hitachi S-2500 SEM, using a Matelect ISM-5 system for signal detection. Measurements were carried out at accelerating voltages ranging from 5 to 20 kV and temperatures between 290 and 410 K. The diffusion length of minority charge carriers (L) and the surface recombination velocity (v_s), were evaluated at different temperatures by fitting EBIC line scans following the method of Kuiken and van Opdorp [7]. CL in the SEM was also used in order to detect extended defects that may influence EBIC measurements. CL observations were performed at 85 K and accelerating voltages from 15 to 25 kV. CL spectra were acquired using a CCD camera with a built-in spectrometer (Hamamatsu PMA-11). AFM measurements were carried out in contact mode using a Park Autoprobe CP microscope.

3. Results and discussion

CL microscopy was used to visualize the defect structure of the epilayer prior to diode fabrication. A representative example of these observations is shown in figure 1. Secondary electron (SE) images usually show smooth surfaces, but some triangular carrot-like defects are also occasionally observed in such micrographs (figure 1(a)). Corresponding panchromatic CL images show a reduced luminescence intensity related to these defects, as shown in figure 1(b). Nevertheless, no changes were observed in the spectral distribution of the associated CL emission (figure 1(c)). The origin of these carrot-shaped ditches in the epilayer is probably perfect screw dislocations pinned at the wafer surface during growth. The dislocation may dissociate into partials, which will propagate in the basal plane and thus form partial ledges in the film [8]. In addition, CL micrographs usually reveal the existence of bigger, triangular, dark areas with sizes up to 200 μm. These triangular areas have been identified as 6H-SiC polytype inclusions by CL spectroscopy. Actually, spectra from defect-free areas (figure 1(c), position 1) show a peak centred at 3.19 eV, corresponding to near-bandgap luminescence of the 4H-SiC polytype, while spectra recorded in the big, dark triangular areas, reveal the existence of another intense emission at 2.93 eV, corresponding to near-bandgap luminescence of the 6H-SiC polytype (figure 1(c), position 2). The simultaneous appearance of both peaks in this and other spectra taken at different accelerating voltages indicates that 6H inclusions were formed at a certain stage of the growth process but subsequently overgrown by the 4H polytype. The formation of this kind of inclusion has been usually associated with generation of extended defects, such as stacking faults, induced by substrate imperfections and growth conditions [9].

EBIC images recorded under different accelerating voltages and beam currents reveal no contrast associated with carrot-like defects or with inclusions. This observation agrees with

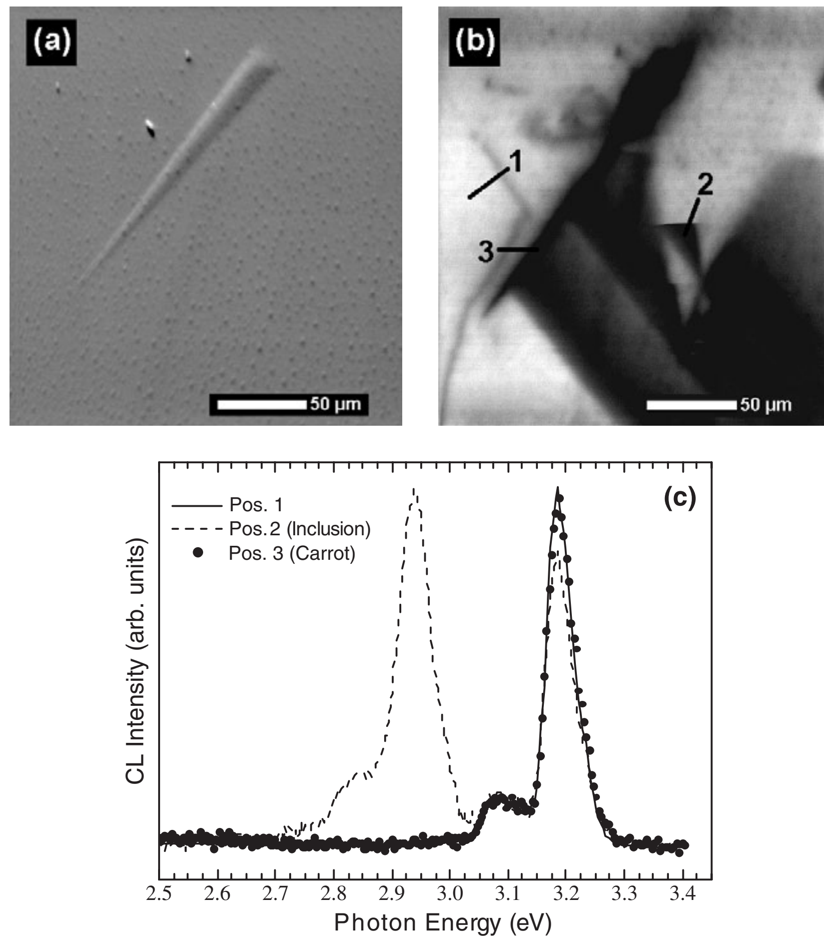

Figure 1. (a) SE image of the 4H-SiC epilayer. (b) Corresponding panchromatic CL micrograph obtained at 85 K using an accelerating voltage of 15 kV. (c) Normalized CL spectra recorded at positions labelled in (b).

previous reports on the absence of detrimental effects in the performance of 4H-SiC diodes due to the presence of the carrot defects mentioned [3]. In contrast, EBIC micrographs (figure 2) show that nanopipes are electrically active defects, appearing as black circles with diameters ranging from 400 nm to 1.5 μm. Changes in the EBIC signal giving rise to the corresponding contrast of such images is about 1 nA. The spatial distribution of the nanopipes was found to be very inhomogeneous. A density of up to 1000 cm^{-2} was estimated in some regions of the investigated material by scanning several areas of about 200 $\times$ 250 μm^2 in size, while the presence of such defects was almost not observed in other zones. The actual size of the nanopipes is smaller than the corresponding black dots appearing in EBIC images and they were not always readily observed in SEM SE images. In order to clearly visualize such defects and to accurately determine their size, AFM was used (figure 3). It was found that the diameter of the nanopipes varied between 250 and 900 nm approximately. The small size of some of these voids suggests that they could correspond to close-cored screw dislocations with small Burgers vectors rather than to the well-known micropipe defects. Micropipes are

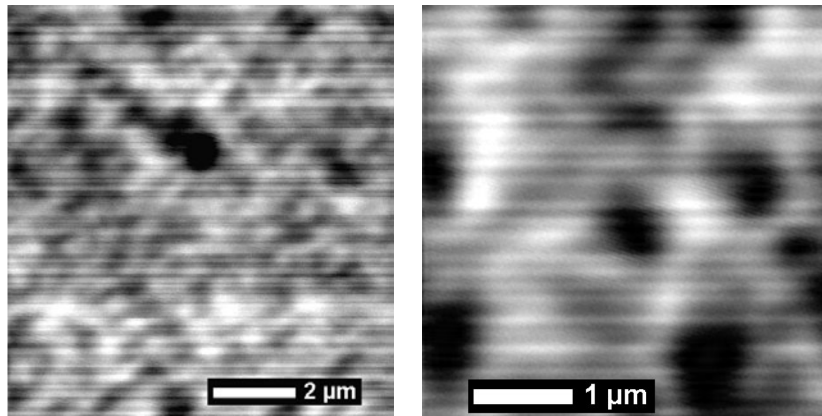

Figure 2. High-resolution EBIC images of the SiC epilayer showing electrically active nanopipes (295 K, 12 kV).

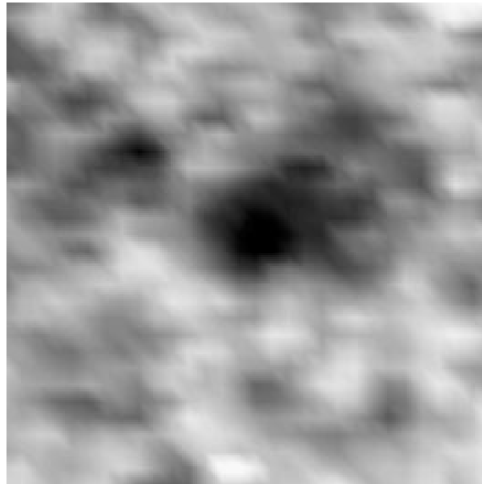

Figure 3. AFM image ($2.4 \times 2.4\ \mu\mathrm{m}^2$) of one of the nanopipes found in the 4H-SiC epilayer.

hollow-core super screw dislocations that run parallel or close to the growth axis and their size usually varies between 0.5 and 30 μm [2, 3]. Both micropipes and closed-cored screw dislocations are recognized to be performance-limiting defects [2, 10, 11]. Actually, the latter are considered responsible for microplasma current fluctuations in diodes under reverse bias, while micropipes constitute a major impediment to the development of large area power devices since they significantly reduce the diode's breakdown voltage.

The minority carrier diffusion length was extracted from EBIC line scans following the method of Kuiken and van Opdorp [7]. If the incident electron beam is perpendicular to the planar Schottky barrier, the EBIC current, I, decays with the beam-to-junction distance, x, according to the relationship

$$I = Ax^{\alpha} \exp(-x/L) \tag{1}$$

where A is constant. In the case of a planar junction, this equation is valid for $x > 2L$. The value of the exponent α depends on the surface recombination velocity v_s and varies between

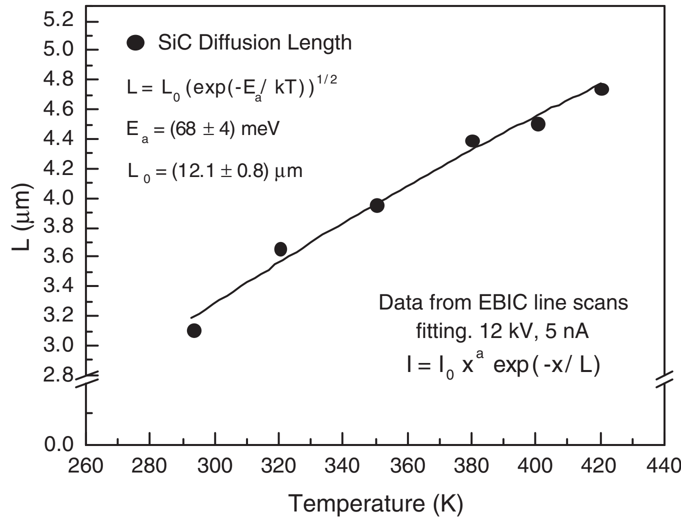

Figure 4. Temperature dependence of the hole diffusion length in the SiC epilayer. The full line represents the fit of the experimental data to equation (2).

$\alpha = -0.5$ for $v_s = 0$ to $\alpha = -1.5$ for $v_s = \infty$. Diffusion length measurements at different temperatures were carried out in defect-free areas, as visualized in EBIC and CL images, using an accelerating voltage of 12 kV and a beam current of 5 nA. For each temperature, several measurements were done in different zones of several diodes and the average value calculated. The difference in diffusion lengths measured under 12 and 20 kV beam voltages did not exceed 10%. No *a priori* assumption was made regarding the surface recombination velocity; both L and α were considered as free parameters in the fitting procedure. Figure 4 present the temperature dependence of the hole diffusion length measured in the 4H-SiC epilayer. Following similar behaviour previously reported for GaAs [12], Si [13] and GaN [14], it is seen that the diffusion length increases for increasing temperature. L values of 3.1 ± 0.2 and 4.8 ± 0.3 μm were respectively estimated at 295 and 420 K. The diffusion length found in this work at room temperature is higher than the previously reported in EBIC studies of 4H- and 6H-SiC diodes [15–17]. A strong decrease of the diffusion length was observed in the proximity of the nanopipes, where L values as low as 200 nm were measured at 295 K. Regarding α, values found for this parameter range between -0.48 and -0.53, which indicates that, in our case, $v_s \approx 0$ [14]. The observed temperature dependence of the diffusion length is in accordance with the Shockley–Read–Hall (SRH) recombination statistics. In the framework of this theory, keeping a fixed injection level, a decrease of L is expected for shallow levels near the band edges when temperature is decreased [18]. This may be interpreted as caused by temperature-induced changes of trap-level occupation [19]. To fit our experimental data the following dependence was used [14, 20]:

$$L = L_0 \exp[(-E_a/kT)]^{1/2} \tag{2}$$

where L_0 is a scaling factor and E_a is the activation energy. The fit, shown in figure 4, was obtained for $L_0 = 12.1 \pm 0.8$ μm and $E_a = 68 \pm 4$ meV. On the basis of the SRH recombination theory, this E_a value gives a donor level at about 0.13 eV below the conduction band edge for the 4H-SiC epilayer investigated here. This E_a value lies between those measured for GaAs (43.5 meV, [20]) and GaN (90 meV, [14]).

EBIC images obtained in cross-section configuration (figure 5) reveal enhanced current collection efficiency in the epilayer, where the doping level is lower. The lines running almost

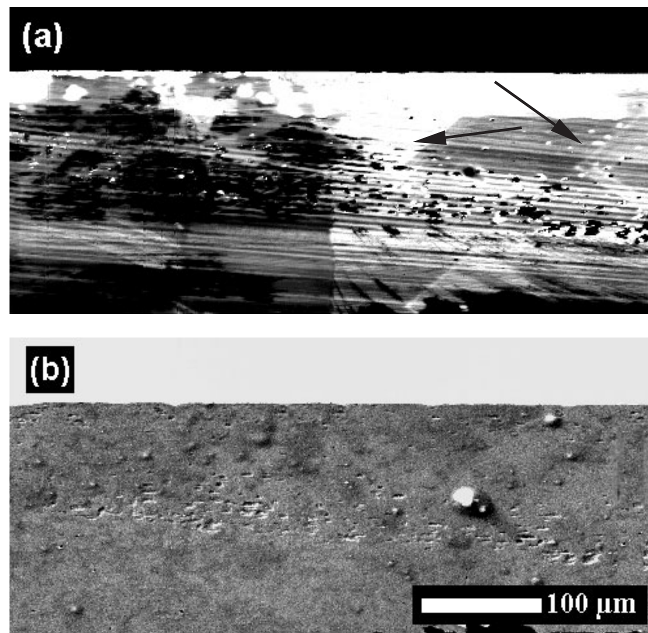

Figure 5. (a) EBIC image of the sample cross section (295 K, 15 kV). The upper white stripe corresponds to the 4H-SiC epilayer. Black arrows mark bright triangular areas that may be related to the presence of stacking faults. (b) Corresponding SE micrograph.

parallel to the edge of the sample, not observed in the corresponding SE images, are probably related to cleaving defects. In addition, bright triangular domains can be appreciated in the right part of the EBIC micrograph (figure 5(a)). The nature of this feature is currently under investigation, but preliminary CL and remote electron-beam-induced current (REBIC) measurements indicate that they are probably related to stacking faults.

4. Conclusions

EBIC has been used to investigate electrically active defects in epitaxial, n-type, 4H-SiC and to measure the hole diffusion length as a function of temperature. The existence of several defects, mainly nanopipes with sizes ranging from 250 to 900 nm, 6H polytype inclusions and triangular, carrot-like, defects, was observed by AFM and CL in a SEM. EBIC images obtained in a planar configuration reveal that only nanopipes are electrically active. Micrographs obtained in a cross-section configuration show an enhanced current collection in the epilayer of the sample. The hole diffusion length (L) was calculated at different temperatures from EBIC line scans recorded in defect-free regions. L values of 3.1 ± 0.2 and 4.8 ± 0.3 μm were respectively estimated at 295 and 410 K, while negligible values of the surface recombination velocity were found. A strong decrease of the diffusion length was observed in the proximity of the nanopipes.

Acknowledgments

This work was supported by MCYT (project MAT2000-2119). Professor F Nava is gratefully acknowledged for providing the material investigated.

References

[1] Matsunami H and Kimoto T 1997 *Mater. Sci. Eng.* R **20** 125
[2] Zimmermann U, Österman J, Kuylenstierna D, Konstantinov A, Vetter W M and Dudley M 2003 *J. Appl. Phys.* **93** 611
[3] Wahab Q, Ellison A, Henry A, Janzén E, Hallin C, Di Persio J and Martínez R 2000 *Appl. Phys. Lett.* **76** 2725
[4] Bhatnagar M, Baliga B J, Kirk H R and Rozgonyi G A 1996 *IEEE Trans. Electron Devices* **43** 150
[5] Kimoto T, Miyamoto N and Matsunami H 1999 *IEEE Trans. Electron Devices* **46** 471
[6] Nava F, Vanni P, Lanzieri C and Canali C 1999 *Nucl. Instrum. Methods* A **437** 354
[7] Kuiken H K and van Opdorp C 1985 *J. Appl. Phys.* **57** 2077
[8] Si W and Dudley M 1997 *J. Electron. Mater.* **26** 151
[9] Konstantinov A O, Hallin C, Pecz B, Kordina O and Janzén E 1997 *J. Cryst. Growth* **178** 495
[10] Neudeck P G, Huang W and Dudley M 1999 *IEEE Trans. Electron Devices* **46** 478
[11] Neudeck P G and Fazi C 1999 *IEEE Trans. Electron Devices* **46** 485
[12] Chernyak L, Lyakhovitskaya V, Richter S, Jakubowicz A, Manassen Y, Cohen S R and Cahen D 1996 *J. Appl. Phys.* **80** 2749
[13] Kittler M, Seifert W, Stemmer M and Palm J 1995 *J. Appl. Phys.* **77** 3725
[14] Chernyak L, Osinsky A, Temkin H, Yang J W, Chen Q and Asif Khan M 1996 *Appl. Phys. Lett.* **69** 2531
[15] Österman J, Hallén A, Jargelius M, Zimmermann U, Galeckas A and Breitzholtz B 2000 *Mater. Sci. Forum* **338–342** 777
[16] Tabib-Azar M, Hubbard S M, Schnabel C M and Bailey S 1998 *J. Appl. Phys.* **84** 3986
[17] Kuznetsov N *et al* 2000 *Mater. Sci. Forum* **338–342** 229
[18] Kittler M and Seifert W 1993 *Phys. Status Solidi* a **138** 687
[19] Kittler M, Seifert W and Schröder K W 1986 *Phys. Status Solidi* a **93** K101
[20] Eckstein M and Habermeier H-U 1991 *J. Physique Coll.* **1** 23